Surface Morphology and Electronic Properties of Dislocations in AlGaN/GaN Heterostructures

J.W.P. HSU,[1,3] M.J. MANFRA,[1] D.V. LANG,[1] K.W. BALDWIN,[1] L.N. PFEIFFER,[1] and R.J. MOLNAR[2]

1.—Bell Laboratories, Lucent Technologies, Murray Hill, NJ 07974. 2.—Massachusetts Institute of Technology, Lincoln Laboratory, Lexington, MA 02420-9108. 3.—e-mail: jhsu@lucent.com

Scanning force microscopy was used to examine the surfaces of AlGaN/GaN heterostructures grown by molecular beam epitaxy (MBE) on GaN templates prepared by hydride vapor phase epitaxy (HVPE). Away from dislocations, the MBE growth replicates the surface morphology of the HVPE film, with monolayer steps clearly visible in topographic images. However, the surface morphology near dislocations depends strongly on the MBE growth conditions. Under Ga rich growth the dislocations appear as hillocks, while under stoichiometric growth they appear as pits. A dependence on Al concentration is also observed. Surface contact potential variation near dislocations is consistent with excess negative charges surrounding by a depletion region, but this was observed only for the film grown under stoichiometric conditions.

Key words: AlGaN/GaN heterostructures, dislocations, surface morphology, surface contact potential

The AlGaN/GaN heterstrostructures with its intrinsic two-dimensional electron gas (2DEG) is a promising materials system for high speed, high power, and high temperature electronics. Recently, it has been shown that the electron mobility (μ) of the 2DEG can exceed 50,000 cm^2/Vs at low temperatures.[1,2] Based on what is known about the 2DEG system in AlGaAs/GaAs heterostructures, growth morphology and interface roughness could have a dramatic impact on the transport properties of the 2DEG.[3] In the AlGaN/GaN system, due to the lack of suitable substrates, dislocations and their associated electronic states present additional factors that can affect surface morphology and 2DEG transport.[4] Hence, it is important to understand how surface morphology correlates with growth conditions and the 2DEG transport properties. Due to its sub-nanometer lateral and vertical resolution, scanning force microscopy (SFM) or atomic force microscopy has become an indispensable tool for surface characterization. For thin film growth, SFM images can be used to evaluate film quality, to distinguish between two-dimensional vs. three-dimensional (island) growth modes, and to discern the existence of defects such as grain boundaries and dislocations. Dislocation mediated surface morphology of GaN films has been thoroughly studied using SFM.[5] In this paper, we use SFM to study how growth conditions and Al concentration influence the surface morphology of AlGaN/GaN heterostructures with high 2DEG mobility. We also apply scanning Kelvin probe microscopy (SKPM) to examine the electronic properties associated with dislocations.

The AlGaN/GaN heterostructures were grown by nitrogen plasma assisted molecular beam epitaxy (MBE) on GaN templates prepared by hydride vapor phase epitaxy (HVPE). The fast growth rate of HVPE produces thick GaN films with reduced threading dislocation densities. The thick HVPE films are ideal substrates for fabricating high quality devices by MBE growth. In this study, all templates were nominally 20 μm thick with a typical threading dislocation density of ~5×10^8 cm^{-2}.[6] The MBE layers consist of a 0.5 μm undoped GaN buffer layer capped by 30 to 40 nm of $Al_xGa_{1-x}N$. All except one sample (#419) were grown under Ga-rich conditions, with clearly observable Ga droplets on the surfaces. Sample #419 was grown under stoichiometric conditions: the surface is smooth but free of Ga droplets. The Al concentration, thickness of AlGaN layer, as well as the electrical properties of the heterostructures in the SFM study are listed in Table I.

All SFM images shown were taken using the tap-

(Received June 25, 2000; accepted November 14, 2000)

Table I. The Aluminum Concentration, Thickness of AlGaN Layer, and Electrical Properties of the Heterostructures in the SFM Study

Sample	Al%	d_{AlGaN} (nm)*	Ga droplets	μ (cm^2/Vs)#	n_s (cm^{-2})#
#419	15	28 (30)	No	9,000	6.5×10^{12}
#512	15	34 (32)	Yes	8,000	6.3×10^{12}
#502	9	27 (27)	Yes	20,000	2.7×10^{12}
#529	6	23 (≤ 40)	Yes	28,000	1.9×10^{12}

* The values of d_{AlGaN} were determined from C-V profiling assuming the 2DEG is at the AlGaN/GaN interface; the numbers in parentheses are the nominal AlGaN thickness according to growth rate.
# μ and n_s were measured at 4.2 K.

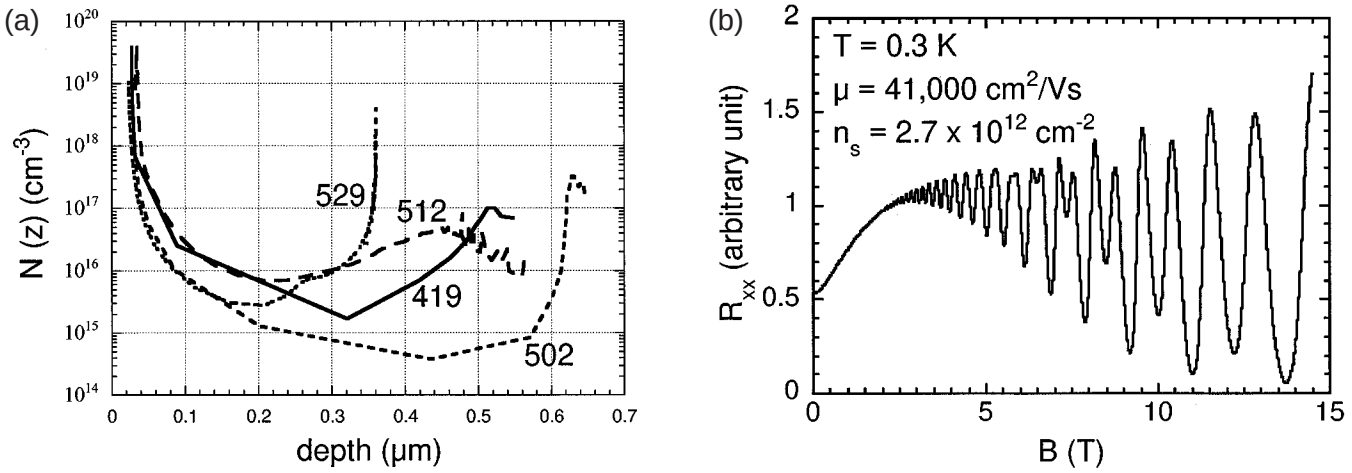

Fig. 1. (a) C-V dopant profiles of samples listed in Table I taken at 100 kHz. The existence of the 2DEG is evident in every sample by the high density near the surface. The carrier density in the HVPE template is ~1.3×10^{17} cm^{-3}. Carrier density increases near the MBE/HVPE interface in every case. (b) Longitudinal magnetoresistance curve taken at 0.3 K for a similarly grown sample with μ = 41,000 cm^2/Vs and 2DEG density $n_s = 2.7 \times 10^{12}$ cm^{-2}.

ping mode. SKPM is a derivative of SFM using conducting tips. Direct current (dc) and alternative current (ac) bias voltages were applied to the tip to measure the electrostatic force between the tip and the sample. To minimize the topographic effect, a topographic trace was first acquired, then the electrostatic force was measured with the tip at 10 nm above the sample surface,[7] but following the previously recorded topographic trace. The external bias voltage produces tip oscillations at the ac bias frequency (ω_{ac}) as well as $2\omega_{ac}$. The ω_{ac} signal depends on the potential difference between the tip and the sample.[8] This experiment was done under closed loop conditions, where a dc bias was applied to the tip to null out the signal at ω_{ac}. This dc bias is then equal to the surface contact potential (SCP) difference between the tip and the sample.[9] Since the tip does not change in a scan, the variation observed in an SCP image reflect the potential variation on the surface. The sources of these potential variation include work function changes, trapped charges, and carrier concentration differences.

Figure 1a shows the 2DEG and the net donor density vs. depth (from surface) derived from capacitance-voltage (C-V) profiles taken at 100 kHz. The high density near the surface is the 2DEG and is clearly evident in all samples. The background net donor density (N_D–N_A) in the undoped MBE GaN layers is extremely low. In one case (#502), N_D–N_A is only 5×10^{14} cm^{-3}. N_D–N_A rises up to ~10^{17} cm^{-3} at MBE/HVPE interface, consistent with 1.3×10^{17} cm^{-3} obtained from direct measurement on the GaN template. In many cases, the MBE/HVPE interface is not abrupt, indicating diffusion of impurities from the HVPE templates into the MBE layer during growth. Figure 1b depicts the low temperature (T = 0.3 K) longitudinal magnetoresistance (R_{xx}) data for a similarly grown $Al_{0.09}Ga_{0.91}N$/GaN heterostructure (μ = 41,000 cm^2/Vs and 2DEG density $n_s = 2.7 \times 10^{12}$ cm^{-2}). The deep modulations of R_{xx} and the low field (~2 T) onset of the Shubnikov-de Haas oscillations clearly point to the high quality of the sample.[2]

Figure 2 shows the differences in surface morphology resulting from changing the III/V ratio. The surface of sample #419 (Fig. 2a), which was grown under stoichiometric conditions, contains small pits in the middle of mounds and some hexagonal shaped depressions (lateral diamter = 50 to 100 nm, depth = 15 to 25 nm). The pit density (~5×10^8 cm^{-2}) agrees well with the dislocation density in the HVPE templates. The pits may result from growth rate variation near dislocations. Dislocations that manifest as pits

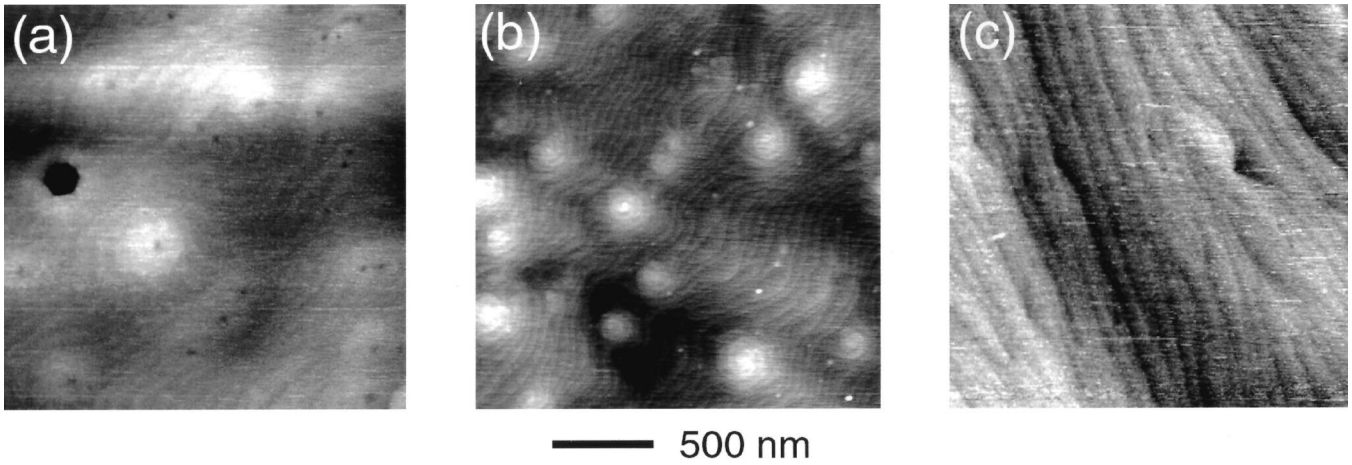

Fig. 2. 2 μm × 2 μm topographic images of (a) #419, (b) #512, and (c) HVPE GaN template. The grayscale and rms roughness are (a) 7 nm and 1.0 nm, (b) 4 nm and 0.5 nm, and (c) 5 nm and 0.45 nm, respectively.

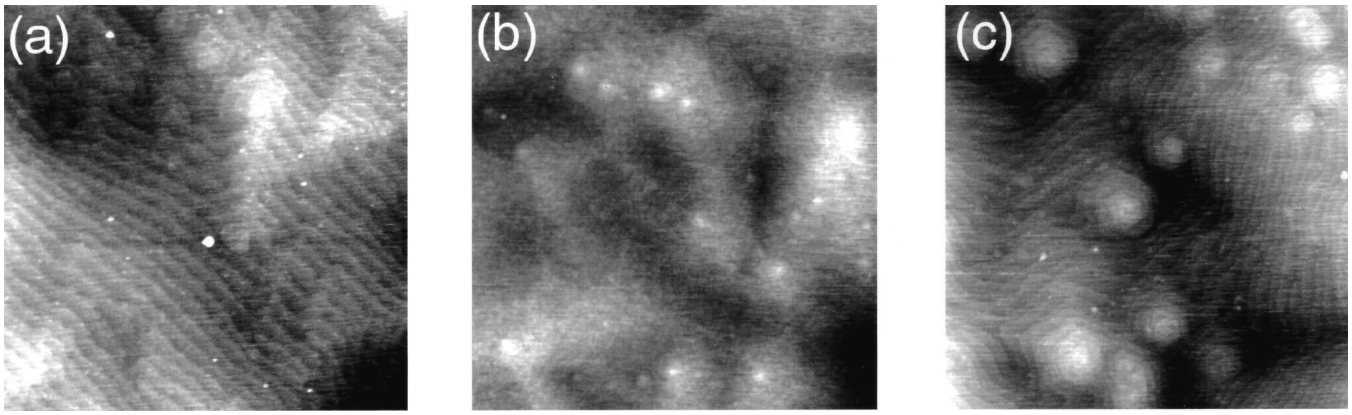

Fig. 3. 2 μm × 2 μm topographic images of (a) #529 (Al = 6%), (b) #502 (Al = 9%), and (c) #512 (Al = 15%). The grayscale and rms roughness are (a) 4 nm and 0.62 nm, (b) 4 nm and 0.84 nm, and (c) 5 nm and 0.72 nm, respectively.

on the surface have been reported in GaN[10] as well as other systems.[11] However, we observe no pits on the surface of Sample #512 (Fig. 2b), which was grown under Ga-rich conditions. Instead, there are hexagonal hillocks with densities ~4.6×10^8 cm^{-2}. We believe these hillocks are centered at dislocations. Thus, the MBE growth rate is apparently reduced near dislocations under stoichiometric conditions and enhanced near dislocations under Ga-rich conditions. Our SFM results on the AlGaN surfaces agree well with previous SFM studies of dislocation mediated GaN surface morphology, which reported that dislocations appear as hexagonal hillocks with high III/V ratios and pits with low III/V ratios in the MBE growth.[5,10] The fact that the morphology on AlGaN surfaces is similar to that on GaN suggests that the AlGaN surface morphology might be determined by the underlying GaN buffer morphology. Away from the dislocations, both samples show clear monolayer steps that replicate the underlying HVPE GaN templates (Fig. 2c). Similar to MOCVD grown GaN films, steps on the HVPE GaN films are mostly straight. Samples #419 and #512 have similar Al concentration and AlGaN thickness. The resulting 2DEG n_s and μ are comparable, indicating that although small variation in growth conditions can affect surface morphology, they do not seem to affect transport characteristics dramatically in this range of μ and n_s.

Figure 3 shows the influence of Al concentration on the surface morphology near dislocations. It appears that the dislocation hillocks are more pronounced with higher Al concentrations. In the lowest Al concentration sample (#529, Fig. 3a), there are no obvious surface features (pits or bumps) that we can associated with dislocations. In the intermediate Al concentration sample (#502, Fig. 3b), the dislocations appear as small round bumps. In the highest Al concentration sample (#512, Fig. 3c), the dislocations become hexagonal hillocks. The fact that the dislocation surface morphology depends on Al concentration indicates that the AlGaN surface morphology is not entirely determined by the GaN buffer. However, we do not know whether this is the intrinsic surface morphology or variation in oxide thickness. It is well known that AlGaAs appears higher than GaAs because of the thicker native oxide in AlGaAs.[12] Since the surface oxide of AlGaN is mostly Al-oxide,[13] dislocations would appear as bumps if the Al concentration is higher near dislocations.

To investigate the electrical properties associated

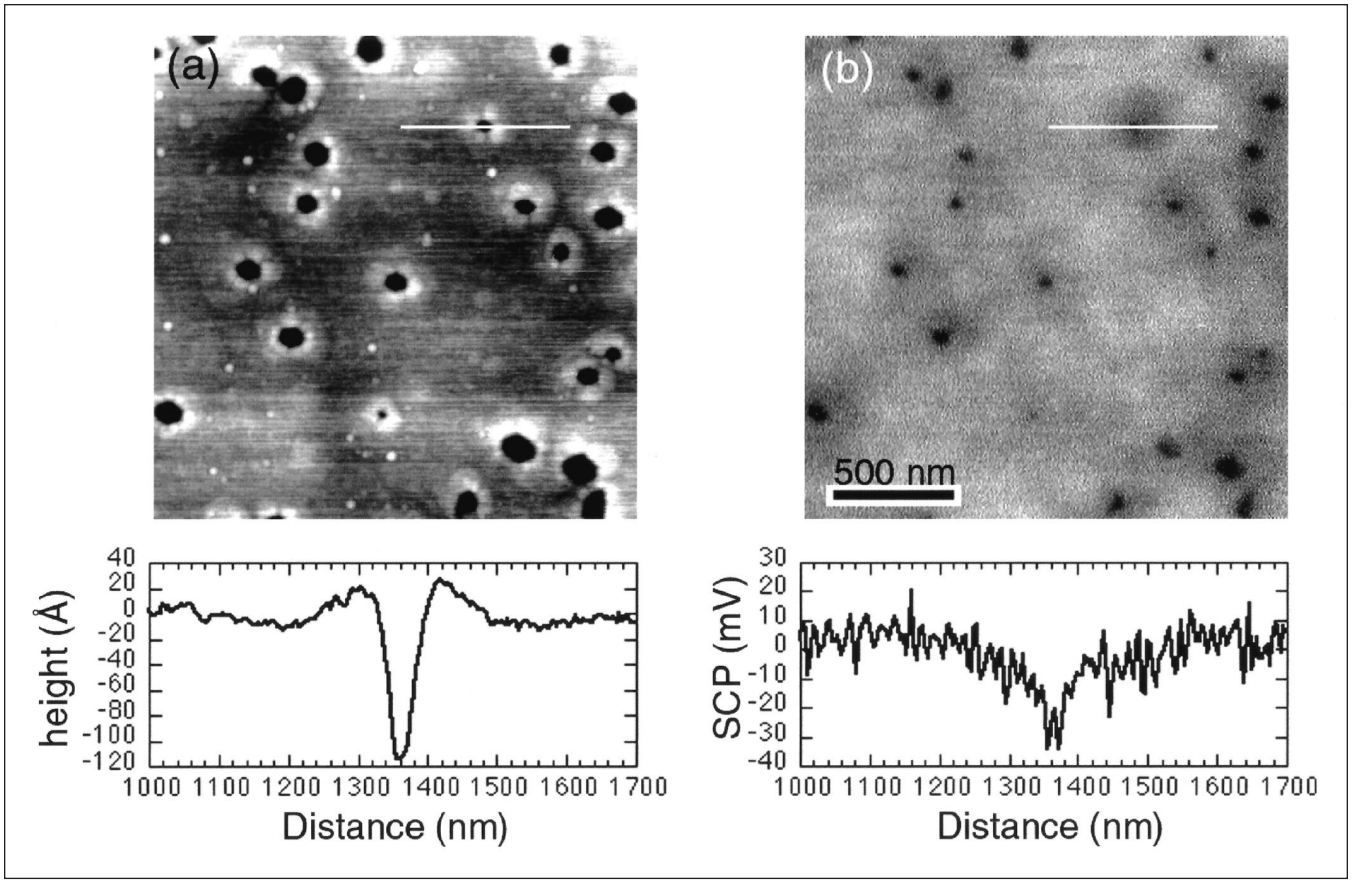

Fig. 4. 2 μm × 2 μm (a) topographic and (b) SCP image of #419 taken at the same sample position. The grayscale represent 8 nm in (a) and 0.1 V in (b). Line cuts across a dislocation indicated in the images are shown below the corresponding image. The topographic profile shows a depression surrounded by a slightly raised area. The SCP profile is cusp like.

with dislocations, we performed SKPM measurements. Figure 4 shows (a) topographic and (b) SCP images of Sample #419 taken at the same sample position. Dislocations in this area of the sample appear as hexagonal pits rather than small dimples in mounds. The SCP is 10 to 30 meV smaller (darker in Fig. 4b) at the dislocations. The dark spots in the SCP images coincide with the pits in Fig. 4a. In addition, the SCP recovers from the reduced values at dislocations to the background at a length scale of ~200 nm. The line cuts in Fig. 4 show the detailed profiles of topographic and SCP changes across the defect indicated in the images. The two profiles are quite different: the topographic profile is volcano-like: depression surrounded by a raised region, while the SCP profile is cusp like.

A lower SCP indicates trapped negative charges at the dislocations. Theoretical investigations indicate that dislocations in n-type GaN contain acceptors below the Fermi level, i.e., they are negatively charged.[14] The presence of excess negative charges at dislocations is also consistent with other experimental results.[15,16] Here we show direct evidence of trapped negative charges at dislocations. Even though there are no free carriers in the AlGaN barrier, the potential associated with the negatively charged dislocation core will be canceled out by the positively charged donors in AlGaN over a certain distance. Using 200 nm as this distance and one electron trapped per c lattice constant (c = 5 Å) at the dislocation core, the corresponding positive charge density equals ~10^{16} cm^{-3}. This value is not unreasonable for N_D–N_A in the AlGaN layer. Curiously, no SCP variation near dislocations was observed for samples grown under Ga rich conditions.

In conclusion, we have shown that MBE growth mostly replicates the morphology of the HVPE GaN templates. These growth conditions produce high 2DEG mobility heterostructures. However, the growth near dislocations is sensitive to small changes in growth conditions and depends on the Al concentration. We also present direct evidence of negatively charged dislocations, but only in the sample grown under stoichiometric conditions.

The Lincoln Laboratory portion of this work was sponsored by the Office of Naval Research under Air Force contract #F19628-00-C-0002. Opinions, interpretations, conclusions, and recommendations are those of the authors and not necessarily endorsed by the United States Air Force.

REFERENCES

1. I.P. Smorchkova, C.R. Elsass, J.P. Ibbetson, R. Vetury, B. Heying, P. Fini, E. Haus, S.P. DenBaars, J.S. Speck, and U.K. Mishra, *J. Appl. Phys.* 86, 4520 (1999).

2. M.J. Manfra, L.N. Pfeiffer, K. West, H.L. Stormer, K.W. Baldwin, J.W.P. Hsu, D.V. Lang, and R.J. Molnar, *Appl. Phys. Lett.* 77, 2888 (2000).
3. e.g., R.L. Willett, J.W.P. Hsu, D. Natelson, K.W. West, L.N. Pfeiffer, cond-mat/0007134 (July 7, 2000).
4. D. Jena, A.C. Gossard, and U.K. Mishra, *Appl. Phys. Lett.* 76, 1707 (2000).
5. B. Heying, E.J. Tarsa, C.R. Elsass, P. Fini, S.P. DenBaars, and J.S. Speck, *J. Appl. Phys. Lett.* 85, 6470 (1999).
6. R.J. Molnar, W. Götz, L.T. Romano, and N.M. Johnson, *J. Cryst. Growth* 178, 147 (1997).
7. The 10 nm was determined by applying an appropriate voltage to the calibrated piezo scanner.
8. Q. Xu and J.W.P. Hsu, *J. Appl. Phys.* 85, 2465 (1999).
9. E.M. Nonnenmacher, M.P. O'Boyle, and H.K. Wickramasinghe, *Appl. Phys. Lett.* 58, 2921 (1991).
10. E.J. Tarsa, B. Heying, X.H. Wu, P. Fini, S.P. DenBaars, and J.S. Speck, *J. Appl. Phys.* 82, 5472 (1997).
11. J.W.P. Hsu, E.A. Fitzgerald, Y.H. Xie, P.J. Silverman, and M.J. Cardillo, *Appl. Phys. Lett.* 61, 1293 (1992).
12. P.A. Rosenthal, E.T. Yu, R.L. Pierson, and P.J. Zampardi, *J. Appl. Phys.* 87, 1937 (2000).
13. T. Hashizume, S. Ootomo, R. Nakasaki, S. Oyama, and M. Kihara, *Appl. Phys. Lett.* 76, 2880 (2000).
14. A.F. Wright and U. Grossner, *Appl. Phys. Lett.* 73, 2751 (1998); J. Elsner, R. Jones, M.I. Heggie, P.K. Sitch, M. Haugk, Th. Frauenheim, S. Oberg, and P.R. Briddon, *Phys. Rev. B* 58, 12571 (1998).
15. N.G. Weimann, L.F. Eastman, D. Doppalapudi, H.M. Ng, and T.D. Moustakas, *J. Appl. Phys.* 83, 3656 (1998); H.M. Ng, D. Doppalapudi, T.D. Moustakas, N.G. Weimann, and L.F. Eastman, *Appl. Phys. Lett.* 73, 821 (1998); D.C. Look and J.R. Sizelove, *Phys. Rev. Lett.* 82, 1237 (1999).
16. P.J. Hansen, Y.E. Strausser, A.N. Erickson, E.J. Tarsa, P. Kozodoy, E.G. Brazel, J.P. Ibbetson, U. Mishra, V. Narayanamurti, S.P. DenBaars, and J.S. Speck, *Appl. Phys. Lett.* 72, 2247 (1998); K.V. Smith, E.T. Yu, J.M. Redwing, and K.S. Boutros, *J. Electron. Mater.* 29, 274 (1999).